# Prophylactic IL-23 blockade uncouples efficacy and toxicity in dual CTLA-4 and PD-1 immunotherapy

Mingyi Ju [1,2], Jiaojiao Zhang,[1,2] Zhuoyuan Deng,[1,2] Minjie Wei,[1,2,3] Lianghua Ma [4], Ting Chen,[5] Lin Zhao[1,2]

**Correspondence to**
Professor Lin Zhao;
lzhao@cmu.edu.cn

Dr Ting Chen;
chenting88726@163.com

Lianghua Ma; sy_mlh@qq.com

## ABSTRACT

**Background** Immune-related adverse events (irAEs), characterized by targeted inflammation, occur in up to 60% of patients with melanoma treated with immune checkpoint inhibitors (ICIs). Evidence proved that the baseline peripheral blood profiles of patients at risk for severe irAEs development paralleled clinical autoimmunity. Interleukin (IL)-23 blockade with risankizumab is recommended for cases that are suffering from autoimmune disease, such as autoimmune colitis. However, currently, the role of IL-23 in irAEs onset and severity remains poorly understood.

**Methods** The pro-inflammatory cytokines most associated with severe irAEs onset were identified by retrospective analysis based on GSE186143 data set. To investigate the efficacy of prophylactic IL-23 blockade administration to prevent irAEs, refer to a previous study, we constructed two irAEs murine models, including dextran sulfate sodium salt (DSS)-induced colitis murine model and a combined-ICIs-induced irAEs murine model. To further explore the applicability of our findings, murine models with graft-versus-host disease were established, in which Rag2$^{-/-}$Il2rg$^{-/-}$ mice were transferred with human peripheral blood mononuclear cells and received combined cytotoxic T-lymphocyte associated antigen 4 (CTLA-4) and programmed cell death protein-1 (PD-1) treatment. Human melanoma cells were xenografted into these mice concomitantly.

**Results** Here we show that IL-23 was upregulated in the serum of patients suffering from irAEs after dual anti-CTLA-4 and anti-PD-1 treatment, and increased as a function of irAEs severity. Additionally, Augmented CD4$^+$ Tems may preferentially underlie irAEs onset. Treating mice with anti-mouse IL-23 antibody concomitantly with combined CTLA-4 and PD-1 immunotherapy ameliorates colitis and, in addition, preserves antitumor efficacy. Moreover, in xenografted murine models with irAEs, prophylactic blockade of human IL-23 using clinically available IL-23 inhibitor (risankizumab) ameliorated colitis, hepatitis and lung inflammation, and moreover, immunotherapeutic control of tumors was retained. Finally, we also provided a novel machine learning-based computational framework based on two blood-based features—IL-23 and CD4$^+$ Tems—that may have predictive potential for severe irAEs and ICIs response.

**Conclusions** Our study not only provides clinically feasible strategies to dissociate efficacy and toxicity in

## WHAT IS ALREADY KNOWN ON THIS TOPIC

⇒ Up to 60% of patients with cancer treated with immune checkpoint inhibitors (ICIs) experience severe immune-related adverse events (irAEs), which involve inflammation in healthy tissues. IrAEs pose a significant obstacle in the creation of a diverse multiagent immunotherapy plan that is necessary to combat the heterogenous and treatment-resistant tumor microenvironment.

⇒ Early recognition and intervention are critical for severe irAEs, which has fueled intensive efforts to unveil what drives the irAEs, which is not only relevant for ICIs implementation, but also provides therapeutic strategies to treat irAEs better. However, a well-tolerated and effective treatment for the prevention of irAEs onset in clinical practice is still lacking.

## WHAT THIS STUDY ADDS

⇒ Interleukin (IL)-23 concentrations were markedly elevated in the serum of patients with irAEs compared with those without.

⇒ Augmented CD4$^+$ Tems, broadly reflected in the bulk transcriptome, single-cell profiles from peripheral blood and mice models with ICIs-induced irAEs, may preferentially underlie irAEs onset.

⇒ Prophylactic blockade of IL-23 ameliorated hepatitis, myocarditis, splenitis, and lung inflammation colitis induced by dual cytotoxic T-lymphocyte associated protein 4 and programmed cell death protein-1 immunotherapy in irAEs murine models, and moreover, did not impair the antitumor effects.

⇒ A machine learning-based computational framework based on two blood-based features—IL-23 and CD4$^+$ Tems—may have predictive potential for severe irAEs, ICIs response and autoimmune disease.

## HOW THIS STUDY MIGHT AFFECT RESEARCH, PRACTICE OR POLICY

⇒ Our study not only provides clinically feasible strategies to dissociate efficacy and toxicity in the use of combined ICIs for cancer immunotherapy, but also develops a blood-based biomarker that makes it possible to achieve a straightforward and non-invasive, detection assay for early prediction of irAEs onset.

the use of combined ICIs for cancer immunotherapy, but also develops a blood-based biomarker that makes it possible to achieve a straightforward and non-invasive, detection assay for early prediction of irAEs onset.

## BACKGROUND

Despite the remarkable progress achieved in cancer therapy through the utilization of immune checkpoint inhibitors (ICIs), around 60% of patients with cancer presently experience immune-related adverse events (irAEs).[1] IrAEs are common, with a low-grade (grades 1–2) effect observed in up to more than 90% of patients, while more severe effects (grades 3–5) can range from 20% to 60%.[2 3] In the most extreme situations, severe irAEs can result in the discontinuation of anticancer therapy, posing a threat to both life and organs.[1 4 5] In all cases, early recognition and intervention are critical for severe irAEs. However, a well-tolerated and effective treatment for the prevention of irAEs onset in clinical practice is still lacking.

Targeted inflammation in otherwise healthy tissues is often characteristic of severe immune-related irAEs, ranging from rashes, arthritis, endocrinopathies, enteropathy, and pneumonitis.[6 7] Therefore, more and more researchers focus on inflammatory factors to ameliorate irAEs associated with ICIs treatment. For example, Yared Hailemichael *et al* found that excessive interleukin (IL-6) release was associated with ICIs-induced toxicity, and blockading IL-6 abrogated immunotherapy toxicity and promoted tumor immunity.[8] Elisabeth Perez-Ruiz *et al* reported that prophylactic blockade of tumor necrosis factor (TNF) before the start of dual anti-cytotoxic T-lymphocyte associated protein 4 (CTLA-4) and anti-programmed cell death protein-1 (PD-1) therapy prevents irAEs in mouse models.[9] The fraction of irAEs stemming from an underlying autoimmune disorder has been not yet clear. Some retrospective reviews of patients with advanced melanoma with pre-existing autoimmune disorders showed that some of the patients experienced a worsening of their pre-existing autoimmune condition requiring treatment following ICI immunotherapy.[10 11] Indeed, Alexander Lozano *et al* recently unveiled that the baseline peripheral blood profile of patients at risk for severe irAEs development paralleled clinical autoimmunity.[12] IL-23 blockade with risankizumab is recommended for cases that are suffering from autoimmune disease, such as autoimmune colitis.[13] Gargiulo, Luigi *et al* present the case of a 28-year-old man diagnosed with stage IV non-BRAFV600E mutated melanoma, who was suffering a severe flare of plaque psoriasis after receiving pembrolizumab treatment. Interestingly, pembrolizumab-induced plaque psoriasis was successfully treated with risankizumab as a clinically available IL-23 inhibitor.[14] This result gives us the light to study the application of IL-23 in the irAEs treatment. However, currently, the role of IL-23 in irAEs remains poorly understood.

Recently, several studies have investigated potential biomarkers for irAEs based on bulk transcriptome or single-cell profiles from peripheral blood or tumor samples. For example, Lim *et al* developed the CYTOX score consists of 11 circulating cytokines with moderately predictive power for severe irAEs in patients with melanoma (area under the curve (AUC)=0.68).[15] Regardless of the moderately predictive power of these cytokines, the detection of 11 circulating cytokines itself not only increases the technical difficulty for clinical application, but also makes the high cost an inevitable limiting factor for wide application. Ying Jing *et al* identified a bivariate regression model of LCP1 and ADPGK that can accurately predict irAEs using The Cancer Genome Atlas (TCGA) database.[16] However, these biomarkers were indirectly discovered through the TCGA database, which does not have toxicity annotations, or were assessed in a case–control scenario without considering low-grade irAEs. A different team discovered that the development of severe irAEs[12] was linked to two pretreatment factors in the bloodstream: the abundance of activated CD4 memory T cells and the diversity of T-cell receptor (TCR). However, their study only stayed at a stage of bioinformatics prediction based on retrospective analysis, without providing strong experimental support and proposing corresponding effective solutions. Given the above, an unmet clinical need still exists for excavating a novel feature correlated with ICIs-induced irAEs onset, and proposing an effective treatment strategy for irAEs.

In this study, we conducted comprehensive clinical, translational, preclinical analyses and established murine models with irAEs to unveil the role of IL-23 in the onset and severity of irAEs. Moreover, we also developed an integrative biomarker to predict irAEs and ICIs response for patients with cancer based on peripheral immune populations.

## METHODS
### Patient data
Data on clinical details and gene expression profiles measured as transcripts per million of peripheral blood mononuclear cells (PBMCs) from patients with metastatic melanoma and prior to starting therapy with either anti-PD-1 blockade (nivolumab or pembrolizumab) or a combination of immune checkpoint blockade (nivolumab targeting PD-1 and ipilimumab targeting CTLA-4) based on GSE186143 data set were used in this study. Severe irAEs were identified by classifying all adverse events using the Common Terminology Criteria for Adverse Events V.5.0 from the US Health and Human Services. Only patients with irAEs grade ≥3 were included. In total, there were 60 samples involved in this work, including 39 no severe irAEs patients and 21 severe irAEs, and 53 samples had complete clinical information. The corresponding TCR single-cell RNA sequencing (scRNA-seq) were obtained from the GSE189126 data set.

Additionally, to verify our findings in a patient group with scRNA-seq data, we also downloaded scRNA-seq profiles of patients who experienced ICIs therapy with or without irAEs from the GSE210037 data set.

Bulk peripheral blood transcriptomes of patients with either systemic lupus erythematosus (SLE) or inflammatory bowel disease (IBD) were obtained from GSE72509 data set and GSE100833 data set, respectively.

The list of these immunotherapy response data sets is displayed in online supplemental table S1.

Human blood samples were obtained from 10 patients with grade 1–2 colitis, who underwent treatment at the Department of Gastroenterology of the First Hospital of China Medical University. Another 10 control blood samples were derived from 10 healthy individuals.

### Cell lines and cell culture

The melanoma cell line B16.BL6 and A357 was provided by Cell Bank/Stem Cell Bank, Chinese Academy of Sciences, and was cultured in Dulbecco's Modified Eagle's Medium (Invitrogen, USA), supplemented with 10% fetal bovine serum (PAA, Germany) at 37°C with 5% $CO_2$ atmosphere. In this study, all of the cells were determined for the absence of *Mycoplasma* contamination.

### Mouse models

The experiments were conducted a minimum of three times, yielding comparable outcomes. Mice were randomized at the beginning of each experiment and experiments were not blinded. Mice were put to sleep once the tumor size exceeded or equaled $200\,mm^2$. Kaplan-Meier estimates were used to plot survival curves, which were then compared through log-rank analysis. The average±SEM is used to express all results.

### Establishment of DSS-induced colitis murine model

We established the mouse model with reference to the method reported by Elisabeth Perez-Ruiz *et al.*[9] Specifically, 6-week-old female C57BL/6J mice were obtained from the Beijing HFK Bio-Technology and maintained in the animal facility of China Medical University. Mice were orally administered 3% dextran sulfate sodium salt (DSS) (MP Biomedicals) in their drinking water for 3 days to induce acute colitis. $2\times10^5$ B16.BL6 melanoma cells were injected subcutaneously into the right subaxillary of 7-week-old female C57BL/6J mice. Anti-CTLA-4 (InVivoMAb Bio X Cell; anti-mouse CTLA-4, clone 9D9) and anti-PD-1 antibody (InVivoMAb Bio X Cell; anti-mouse PD-1, clone RMP1-14) or IgG isotype were injected intraperitoneally at a dose of $100\,\mu g$ per mouse. Colitis treatment was used by the intraperitoneal administration of rat anti-mouse IL-23 antibody ($100\,ng$ per mouse; clone G23-8, No. 14–7232; eBioscience). Body weights, diarrhea (stool consistency) and rectal bleeding were daily recorded to calculate the Disease Activity Index (DAI) scores, as previously described.[17] Mice were bled on day 21 for serum collection. The concentrations of murine IL-6, IL-23, IL-24, and IL-32 were quantified by ELISA (R&D Systems). The survival time of another batch of mice was monitored (n=5/group).

### Combined ICIs-induced irAEs murine model

Six-week-old female C57BL/6J mice were obtained from the Beijing HFK Bio-Technology and maintained in the animal facility of China Medical University. The irAEs murine model by only adopting the treatment scheme of anti-PD-1 and anti-CTLA-4 combined administration twice a week for 3 weeks, refer to the method of previous research.[18] C57/BL6 mice were treated intraperitoneally with $200\,\mu g$ anti-mouse PD-1 (InVivoMAb Bio X Cell; anti-mouse PD-1, clone RMP1-14) and $150\,\mu g$ anti-mouse CTLA-4 (InVivoMAb Bio X Cell; anti-mouse CTLA-4, clone 9D9) or the IgG isotype twice a week for 3 weeks, either in combination with $100\,ng$ anti-mouse IL-23 (clone G23-8, No. 14–7232; eBioscience) or without on days 0, 2, 4 and 6. The concentrations of IL-23 of mice in ICIs group before receiving ICIs treated (baseline levels) were quantified by ELISA (R&D Systems). Mice were bled on day 21 for serum collection to evaluate alanine transaminase (ALT) and aspartate transaminase (AST) serum levels (n=10/group).

### Xenograft-induced irAEs murine model

Eight-week-old female $Rag2^{-/-}Il2rg^{-/-}$ mice were obtained from the Shanghai Model Organisms Center and maintained in the animal facility of China Medical University. Mice were inoculated subcutaneously with $5\times10^5$ A375 cells. On day 7 after tumor-cell inoculation, $1\times10^7$ human PBMCs resuspended in $1\,mL$ normal saline were injected intraperitoneally. Human blood samples were obtained from healthy donors, and fresh PBMCs were isolated by density-gradient separation (Ficoll-Paque Plus; Solarbio). Mice were injected intraperitoneally with ipilimumab ($200\,\mu g$/per mouse) and nivolumab ($200\,\mu g$/per mouse) and risankizumab ($100\,\mu g$/per mouse) or IgG ($200\,\mu g$/per mouse) on days 7, 11, 14 and 17. Xenografted tumors were measured every 3 days. Mice were bled on day 21 for serum collection to evaluate ALT and AST serum levels (n=5/group).

### Histopathology of murine samples

Longitudinal incisions were made in colon samples, and the contents were gently removed by flushing with phosphate-buffered saline (PBS). The colon was enveloped in a "Swiss roll" and secured using a solution of 10% formalin. Regularly, tissue samples were transformed into paraffin blocks, cut into 4 micron sections, and then stained using H&E.

### Immune cell isolation from tumors and spleens and flow cytometry analyses

The tumor tissues were cut into small pieces using razors and then treated with $2.5\,mg/mL$ collagenase IV (Sigma) and $0.1\,mg/mL$ DNase I (Sigma) for 2 hours. After that, the reaction was balanced out by adding 10% fetal bovine serum. The cells were washed using roswell park memorial institute (RPMI) /2% fetal bovine serum (FBS) at room temperature by passing them through the strainer. Tumor tissue lymphocytes were concentrated using a

Ficoll gradient (Histopaque 1119; Sigma-Aldrich). To isolate spleen cells, spleens were smashed with a sterile syringe plunger onto a 40 µm cell strainer to generate single-cell suspensions. The manufacturer's recommendations were followed to remove red blood cells using RBC Lysis Buffer (Tonbo Bioscience). The cells were spun at a speed of 600 g for 5 min at a temperature of 4°C. Flow cytometry analyses were performed on 2 million cells. The antibodies described in online supplemental table S2 were used to stain the cell suspensions. Unless otherwise specified, a dilution of 1:200 was used for all antibodies conjugated with fluorochrome. After being washed once more, the cells were resuspended in 400 µL of PBS before being collected and analyzed using a BD Fortessa flow cytometer.

### Assessment of immune cell abundance
To ensure the accuracy of our results, in this work, we used seven methods-TIMER,[19] CIBERSORT,[20] quanTIseq,[21] xCell,[22] MCP-counter,[23] EPIC[24] and ImmuneCell AI[25] to estimate the immune cell infiltrations. To extend the analysis of CD4+ T-cell features associated with irAEs, we further employed single sample gene set enrichment analysis (ssGSEA) to calculate the CD4+ T-cell abundance of patients with or without severe irAEs using immune cells' marker genes (online supplemental table S3).

### Evaluation of tumor immunity and immune-related indicators
To evaluate tumor immunity, we used the Estimation of STromal and Immune cells in MAlignant Tumors using Expression data (ESTIMATE) technique. This method calculates the immune score, stromal score, and ESTIMATE score for every tumor sample, measuring the level of immune activity (immune infiltration level) through the expression of immune genes.[26] ssGSEA algorithm was used to calculate different immune-related indicators (including interferon (IFN) response, cytolytic activity (CYT), human leukocyte antigen (HLA), tumor infiltrating lymphocytes (TILs), innate and adaptive immunity) using their feature genes (online supplemental table S3).

### Construction of a composite model to predict severe irAEs development
To develop a composite model that outperform either feature alone for severe irAEs prediction, we developed a novel machine learning-based computational framework based on a logistic regression framework (glm in R) to train a composite model. 54 patients were randomly split into two groups by a 3:1 ratio. Thus, 37 patients were assigned to the training cohort, and 16 patients were assigned to the test cohort.

The evaluation of composite model scores was conducted through receiver operating characteristic (ROC) analysis. Trained models were used to forecast the occurrence of severe irAEs by distinguishing them from non-severe irAEs. To forecast the occurrence of irAEs, separate validation was conducted for composite models based on therapy type. Additionally, they were compared with biomarkers previously assessed in bulk RNA-seq.

### Survival analysis
We compared the time developed to severe irAEs of patients separated by the median score as the cut-off value. Kaplan-Meier (K-M) curves were carried out to compare the time-to-severe irAEs. P values from log-rank tests were calculated, and less than 0.05 was considered statistically significant.

### Statistical analysis
The data underwent analysis using unpaired t-tests, Kruskal-Wallis test, and One-way analysis of variance when appropriate. Significant differences were determined at a significance level of p<0.05. Using the Spearman's method, we computed the correlation between two variables. A correlation is considered significant if the p value (from Spearman's correlation test) is less than 0.05. We employed C-index analysis to assess the impact of various features on the prediction of severe irAEs. The R package "survivalROC" was used to conduct ROC curves that were dependent on time, and the predictive performance of various features was evaluated by calculating the area under the ROC curve. The statistical analysis was conducted using either GraphPad Prism V.9.0 or SPSS V.19.0 software package. Statistical significance was determined if the two-tailed p value was <0.05.

## RESULTS
### IrAEs were associated with response rate to ICIs treatment
A previous data indicated that the onset of irAEs might serve as a clinical biomarker to predict a favorable therapeutic response to ICIs, while some other studies reported no associations between irAEs and ICIs efficacy.[27] Therefore, we further sought to explore the correlation between response to and ICIs-induced irAEs. We found that all patients with ICIs-induced irAEs demonstrated marked improvements in response rate compared with those lacking toxicity (p=0.0032, online supplemental figure S1A). Moreover, in the PD-1 monotherapy cohort, patients with irAEs tended to achieve higher response rates than those lacking toxicity (p=0.0212, online supplemental figure S1B). However, as for the combination therapy cohort, there was no significant difference in response rates between patients with or without irAEs (p=0.4419, online supplemental figure S1C).

Additionally, as for irAEs severity, patients with severe irAEs (grade 3+) had no significant difference in ICIs response rate compared with those with no severe irAEs in all patients (p=0.3814, online supplemental figure S1D), PD-1 monotherapy (p=0.1017, online supplemental figure S1E) or combination therapy cohorts (p=0.2211, online supplemental figure S1F). Furthermore, patients treated with combination ICIs appear to be more strongly associated with irAEs (p=0.0009, online supplemental figure S1G) or severe irAEs (p=0.0001, online

supplemental figure S1H) onset than those treated with PD-1 monotherapy.

These data indicated that patients with ICIs-induced irAEs tended to obtain higher response rates to ICIs treatment than those without; however, the severity of irAEs was not associated with the ICIs response rate, which provided further evidence support to address the key problem of the controversial relationship between irAEs and ICIs response. Additionally, our findings also filled the gap in the previous evidence that there was no correlation between irAEs and ICIs response in patients treated with anti-CTLA-4 therapy.

### IL-23, as a pro-inflammatory cytokine, has potential for predicting time-to-severe irAEs independent of key clinical variables in melanoma

As an initial approach to understand the critical pro-inflammatory cytokines associated with irAEs development, we used an RNA-seq cohort including 60 pre-therapy blood samples (GSE186143) to comprehensively profile inflammatory gene expression in blood samples from patients with melanoma with ICIs-induced severe irAEs. The schematic diagram is shown in figure 1A. In order to screen the cytokines most closely associated with irAEs development among these 61 pro-inflammatory cytokines, we divided the patients into three groups: no irAEs (grade 0, N=17), low-grade irAEs (grade 1/2, N=22), and severe irAEs (grade 3/4, N=21), and looked for the genes with significant difference of expression between any two groups of these three groups. The results showed that out of the 61 pro-inflammatory cytokines, four genes (IL-6, IL-23, IL-24 and IL-32) showed significant association with irAEs at baseline in blood samples from patients with melanoma. Moreover, among these four genes, IL-23 showed the most significant difference among these three groups, and increased as a function of irAEs severity (Kruskal-Wallis p=0.0270, figure 1B, online supplemental table S4).

To further explore whether these four genes could predict time-to-severe irAEs, we evaluated the predictive power of these four irAEs-related inflammatory genes for severe irAEs using K-M plot analysis. We randomly divided the 53 schematic diagram patients with complete clinical information into train (N=26) and test (N=27) cohort. Patients were assigned to high versus low groups by the median value of expression as the cut-off. For IL-23, patients in the high group experienced severe irAEs after treatment initiation, whereas the vast majority of patients in the low group little experienced a severe irAEs in all of the three cohorts (train cohort: p=0.0072, figure 1C; test cohort: p=0.0036, figure 1D; all cohort: p=0.0352, figure 1E). IL-6, however, does not seem to be related to time-to-severe irAEs. IL-24 and IL-32 demonstrated potential predictive power for severe irAEs only in cohorts 1 and 2, respectively, suggesting unstable power for predicting severe irAEs. In addition, the area under the ROC curve of IL-23 for severe irAEs at 3 years was 0.65, 0.78 and 0.73 in train, test and all cohorts, respectively (figure 1F),

which exhibited moderate classification performance, underscoring its robustness.

To test whether IL-23 could predict time-to-severe irAEs independent of key patient parameters, we further evaluated the AUC value of IL-23 in various patient subgroups according to different clinical characteristics. Indeed, regardless of ICIs therapy type, ICIs response status, age, sex, melanoma subtype or affected organ system, no matter in 1, 3 or 5 years, the model remained predictive (figure 1G).

To investigate which leukocyte type transcribes IL-23, as a severe irAEs-associated gene, in human peripheral blood, we have performed scRNA-seq analysis based on peripheral blood obtained pretreatment from patients with metastatic melanoma treated with immune checkpoint blockade using GSE189125 data set. In this data set, patients were divided into two cohorts named Batch A and Batch B, respectively. Then, patients with severe irAEs were involved in our analysis (Batch A, N=6; Batch B, N=3). The results of scRNA-seq analysis based on Batch A cohort indicated that IL-23 was mainly expressed in monocytes, followed by T cells. To verify this finding, we further evaluate IL-23 expression levels based on Batch B cohort (online supplemental figure S2A–C). Consistent with previous results, the expression of the IL-23 gene was primarily produced by monocytes, followed by B cells and T cells (online supplemental figure S2D–F).

Given the above, we found that IL-23 increased in blood samples from patients with melanoma with ICIs-induced severe irAEs, and has the potential for predicting time-to-severe irAEs independent of key clinical variables. IL-23, as a severe irAEs-associated gene, might mainly source from monocytes in human peripheral blood.

### TCR clonal dynamics relate to expression levels of IL-23 prior to irAEs onset

Evidence showed that the expansion of peripheral blood T-cell clones prior to irAE onset positively correlates with irAEs severity during checkpoint blockade treatment.[28 29] Therefore, we further examine the correlation between IL-23 expression and TCR clonal diversity in peripheral blood samples prior to irAEs using the GSE189126 data set. The results showed that the expression of IL-23 had a markedly positive correlation with TCR clonal diversity both in Shannon entropy (online supplemental figure S3A, R=0.279, p=0.043) and Gini-Simpson index (online supplemental figure S3B, R=0.275, p=0.046). To test the robustness of the correlation between IL-23 expression and TCR clonal diversity, we next assigned patients to high versus low groups according to the median value of IL-23 expression. Patients with high IL-23 expression had more TCR clonal diversity than those with low IL-23 expression, both in Shannon entropy (online supplemental figure S3C, p=0.033) and Gini-Simpson index (online supplemental figure S3D, p=0.044).

Given the above, we wondered whether pretreatment TCR clonotypes in peripheral blood might show a greater propensity to expand in patients with high IL-23
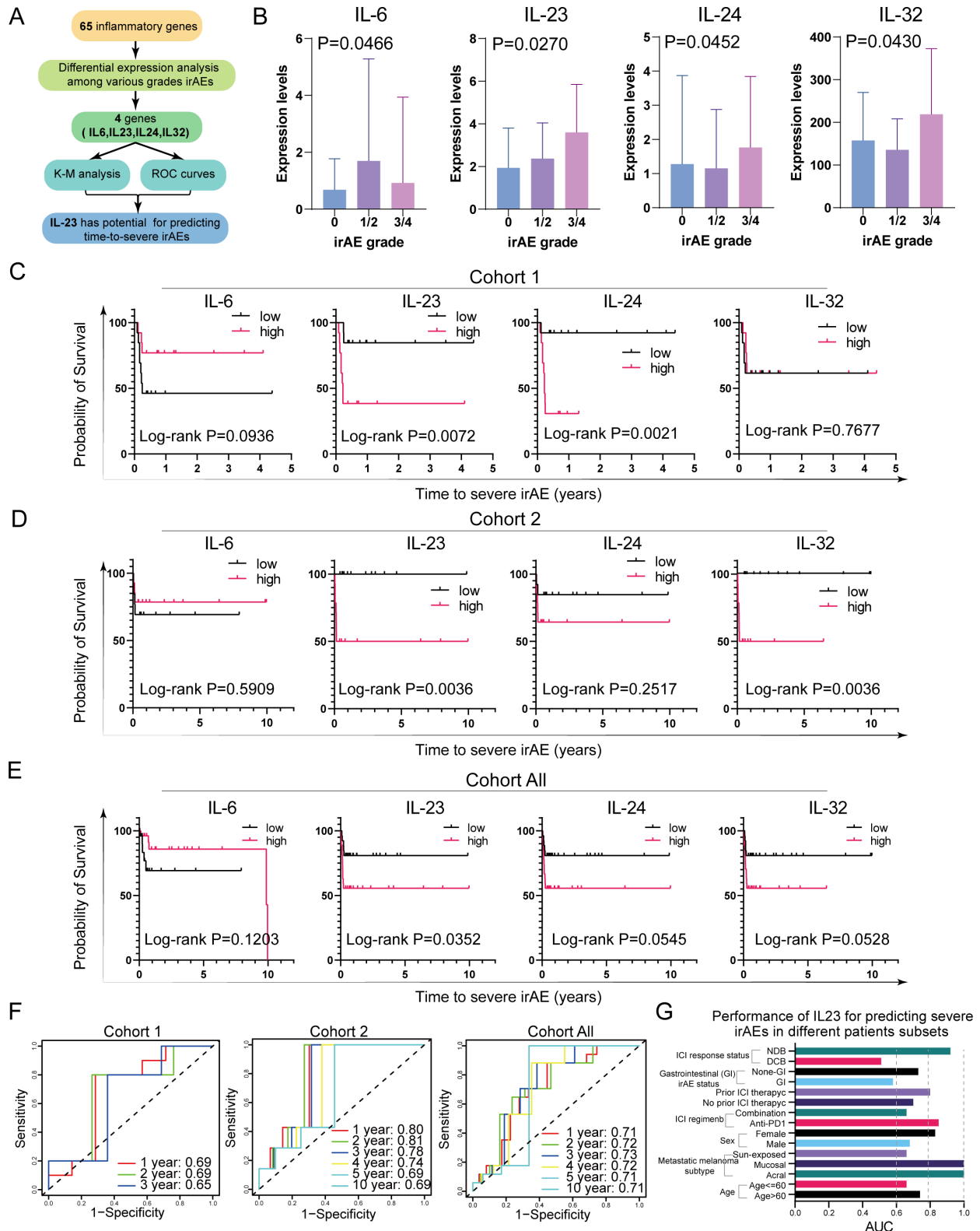
**Figure 1** IL-23 was markedly elevated in blood samples from patients with melanoma with irAEs than those without, and was associated with severe irAEs development. (A) Schematic diagram for gene expression profiling analysis. (B) IL-6, IL-23, IL-24 and IL-32 showed significant increase in patients with severe irAEs compared with those without in the GSE186143 data set. Kaplan-Meier analysis for freedom from severe irAE in cohort 1 (C) cohort 2 (D) and all patients cohort (E) stratified by the cytokine expression levels. (F) ROC plots showing IL-23 performance for predicting time-to-severe irAEs in cohort 1 (left), cohort 2 (middle) and all patients cohort (right). The AUC is shown for each ROC curve. (G) Performance of IL-23 in all patients cohort for predicting severe irAEs in different patient subgroups stratified by key patient parameters. AUC, area under the curve; DCB, durable clinical benefit; GI, gastrointestinal; IL, interleukin; irAE, immune-related adverse event; K-M, Kaplan-Meier; NDB, no durable clinical benefit; ROC, receiver operating characteristic.

expression after ICIs treatment initiation. To unveil this mystery, we profile bulk TCR-β repertoires in paired pretreatment and early on-treatment PBMC samples collected from 15 patients with metastatic melanoma treated with ICIs therapy based on the GSE189126 data set, and used a TCR clonality index that was robust to variation in the number of clones captured (Pielou's evenness[30]). TCR clonal expansion was assessed as measured by an increase in 1–Pielou's evenness. Interestingly, the results showed that both significantly increased TCR clonal expansion and persistence of baseline clones in patients with high IL-23 expression compared with those with low IL-23 expression (online supplemental figure S3E,F), which suggested that TCR clonal dynamics in relation to IL-23 expression in patients treated with ICIs therapy. In addition, we also identified a striking association between the numbers of unique TCR-α and TCR-β clones and IL-23 expression in peripheral blood samples. Specifically, patients with high IL-23 expression possessed more unique TCR-α and TCR-β clones compared with those with low IL-23 expression (online supplemental figure S3G, TCR-α: p=0.053; TCR-β: p=0.036). However, neither the numbers of TCR-γ nor TCR-δ clones within the systemic circulation were significantly different between patients with high IL-23 expression and those with low IL-23 expression (online supplemental figure S3G, p>0.05).

Collectively, these findings suggest that a more diverse TCR repertoire prior to irAEs onset, broadly reflected in bulk peripheral blood, is associated with high expression levels of IL-23.

### Effector memory CD4^{+} T cells markedly augmented in patients with severe irAEs or autoimmune disease compared with controls

IrAEs were indicated to be induced by activation of immune responses unrelated to those targeting the tumor.[2] Therefore, to deeply unveil the severe irAEs-associated immune landscape, we preliminary evaluated the distinctions of the immune-related signatures between the severe and no severe irAEs. Interestingly, we observed that CYT, TILs, immune score and ESTIMATE score significantly ascended in severe irAEs patients compared with those with no severe irAEs (figure 2A). Particularly, for immunity types, adaptive immunity displayed significant enrichment in severe irAEs compared with no severe irAEs. In contrast, differences in innate immunity linked to severe irAE development were less pronounced (figure 2A,B). These results suggest that severe irAEs onset appears to be associated with adaptive immunity rather than innate immunity. Moreover, patients with severe irAEs tended to have lower dysfunction scores of immune cells (p=0.0132, figure 2C) than those with no severe irAEs, which suggests that patients with severe irAEs might have more active immune cells.

We next sought to examine the immune cell infiltrations between patients with or without severe irAEs using seven algorithms. As shown in figure 2D, the top three

categories of immune cell types included those from innate and adaptive immunity. They were CD4^{+} T cells (TIMER), CD4^{+} activated memory T cells (CIBERSORT) and monocytes (CIBERSORT) (online supplemental table S5). Among these immune cells, we can observe that CD4^{+} T cells had the most significant discrepancy between patients with or without severe irAEs, and patients with severe irAEs tended to have more infiltrations of CD4^{+} T cells (figure 2E). Given this, we asked which subpopulation of CD4^{+} T cell was most associated with severe irAEs onset. To this end, we evaluated the infiltrations of CD4^{+} T cells using gene sets derived from the TISIDB database. Remarkably, of 11 CD4^{+} T-cell subpopulations evaluable by ssGSEA, effector memory CD4^{+} T cell, central memory CD4^{+} T cell, naive CD4^{+} T cell and Tr1 showed significant association with severe irAEs development (figure 2F).

Next, we interrogated the predictive potential of each immune cell subpopulation with respect to severe irAEs outcomes. Of all subpopulations, CD4^{+} T cells (TIMER, EPIC) and CD4^{+} activated memory T cells (CIBERSORT-ABS) showed high predictive power for severe irAEs development (AUC>0.8, figure 2G). Moreover, patients with higher infiltrations of CD4^{+} T cells (TIMER, EPIC) and CD4^{+} activated memory T cells (CIBERSORT-ABS) tended to develop severe irAEs sooner (CD4^{+} T cells (TIMER): p<0.0001; CD4^{+} T cells (EPIC): p=0.0001; CD4^{+} activated memory T cells (CIBERSORT-ABS): p<0.0001, figure 2H). To validate the robustness of the predictive power of these immune cells for severe irAEs development, we further applied all subpopulations to the Lasso and SVM algorithm. The overlap of results from these two algorithms demonstrated that only CD4^{+} T cells were significant (figure 2I, online supplemental table S6), again reflecting its strong association with severe irAEs development.

Having identified CD4^{+} T cell as candidate pretreatment determinants of severe irAEs development, we next set out to verify our findings in a patient group with scRNA-seq data (GSE210037). As shown in figure 2J,K, patients with or without irAEs yielded 5,450 and 4,240 cells, respectively. Extended analysis of T-cell features demonstrated that effector memory CD4^{+} T cell, type 17 helper cell and effector memory CD8^{+} T cell were the top three categories with the most significant elevation in patients who experienced irAEs among these T cells (figure 2L). Moreover, CD4^{+} T cell showed the strongest association with irAEs among these T cells, analogous to our findings in the bulk cohort (GSE186143). Collectively, these findings suggested that CD4^{+} T cell, broadly reflected in the bulk transcriptome and single-cell profiles from peripheral blood, might preferentially underlie irAEs, and effector memory CD4^{+} T cell might play the major role among all CD4^{+} T-cell subpopulations. Effective memory CD4^{+} T cells were significantly associated with autoimmune disorders relative to healthy individuals.

Alexander Lozano and colleagues revealed that the initial peripheral blood profile of patients who are at risk of developing severe irAEs closely resembled
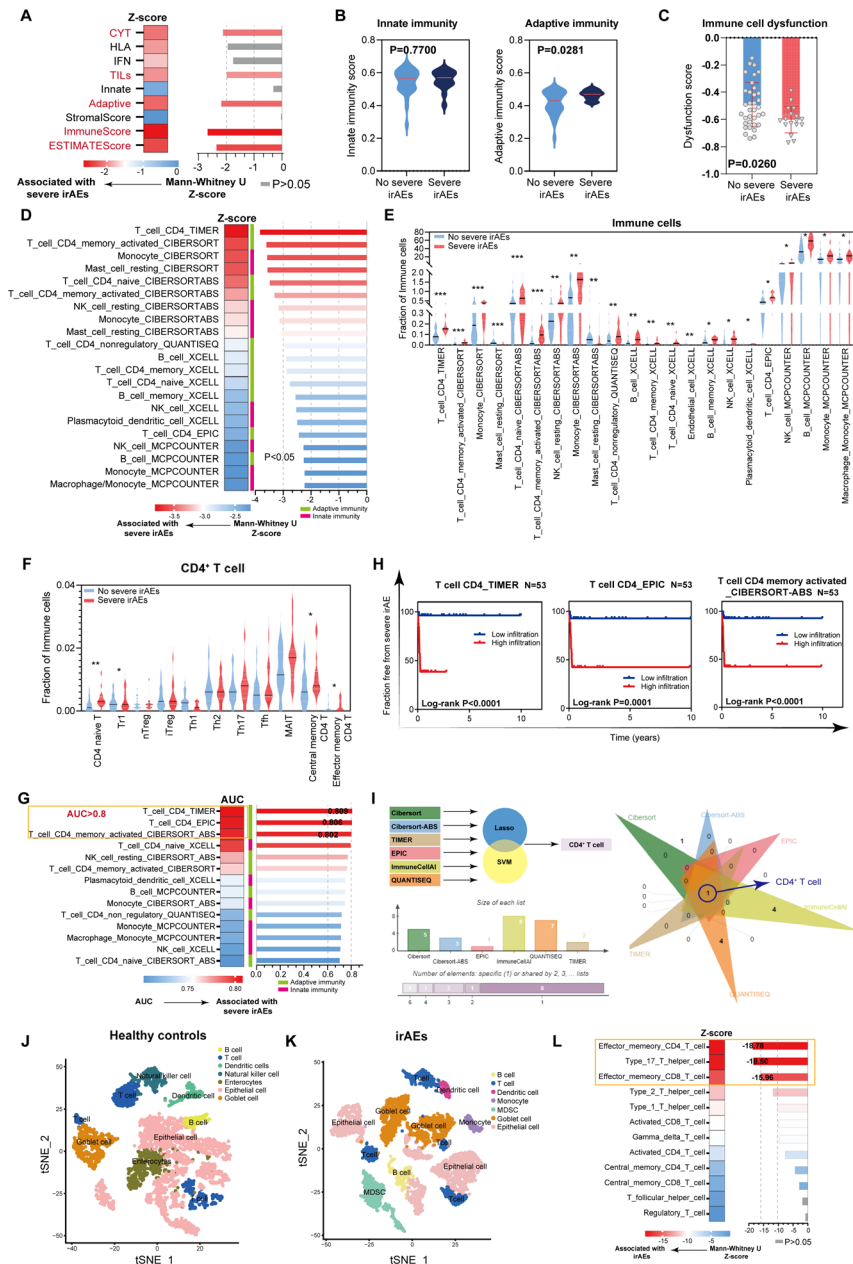
**Figure 2** Immunity characterization of severe irAEs in melanoma using bulk transcriptional and single-cell profiles. (A) Enrichment of relative signatures in patients with severe irAEs compared with those without severe irAEs. Relative signatures were determined by ssGSEA. Significance was determined by a two-sided, unpaired Wilcoxon rank-sum test and integrative meta z-score. (B) The difference between innate immunity (left) and adaptive immunity (right) between severe and no severe irAEs subgroups. (C) The dysfunction score of immune cell in severe and no severe irAEs subgroups. (D) Enrichment of immune cells in patients with severe irAEs compared with those without severe irAEs. Immune cell composition was determined by seven methods-TIMER, CIBERSORT, quanTIseq, xCell, MCP-counter, EPIC and ImmuneCell AI. Significance was determined by a two-sided, unpaired Wilcoxon rank-sum test and integrative meta z-score. (E) The infiltrations of immune cells in patients with melanoma stratified by irAEs severity. (F) The extended analysis of CD4^{+} T cells in patients with melanoma stratified by irAEs severity using ssGSEA. (G) Performance of the immune cell abundance in patients with melanoma for predicting severe irAEs. (H) Kaplan-Meier analysis for freedom from severe irAEs in patients with melanoma stratified by CD4^{+} T cells-TIMER (left), CD4^{+} T cells-EPIC (middle) and CD4^{+} activated memory T cells-CIBERSORT-ABS (right). (I) Left: Strategy of identifying immune cells significantly related to severe irAEs development. Right: Venn diagram showed overlaps of immune cells significantly related to severe irAEs development in various algorithms. *0.01<p<0.05; **0.001<p<0.01; ***p<0.001. Dimensionality reduction (UMAP) of 4,240 pretreatment peripheral blood cells from (J) healthy patients and (K) irAE patients, colored by major cell lineages using single-cell profiles. (L) Enrichment of T cells in patients with irAEs compared with controls. AUC, area under the curve; CYT, cytolytic activity; ESTIMATE, Estimation of STromal and Immune cells in MAlignant Tumors using Expression data; HLA, human leukocyte antigen; IFN, interferon; irAE, immune-related adverse event; MDSC, myeloid-derived suppressor cells; ssGSEA, single sample gene set enrichment analysis; TIL, tumor infiltrating lymphocyte; t-SNE, t-Distributed Stochastic Neighbor Embedding; UMAP, uniform manifold approximation and projection.

clinical autoimmunity.[12] Therefore, to explore whether the CD4+ T-cell abundance of patients at risk for severe irAEs development paralleled clinical autoimmunity, we further evaluated them in bulk peripheral blood transcriptomes spanning two studies and patients with either SLE or IBD relative to healthy controls. Effector memory CD4+ T cells markedly augmented in patients with IBD or SLE compared with healthy controls (IBD-GSE100833: p=0.0209, online supplemental figure S4A; SLE-GSE72509: p<0.0001, online supplemental figure S4B), which paralleled immunity landscape of severe irAEs.

## DSS-induced colitis, exacerbated by anti-PD-1 and anti-CTLA-4, is ameliorated by prophylactic IL-23 blockade

Colitis is among the most frequent and problematic irAEs that are associated with dual checkpoint inhibition.[31] IBD can be modeled in mice by providing DSS in the drinking water.[32] To explore the relationship between IL-23 and irAEs-associated colitis in vivo, we constructed a DSS-induced colitis mice model in which a combination of anti-CTLA-4 and anti-PD-1 monoclonal antibodies was administered to mice receiving DSS (figure 3A). The combination treatment exacerbated the autoimmune colitis syndrome induced by DSS and resulted in decreased body weight (p=0.0026, figure 3C), increased DAI score (p=0.0130, figure 3D) and shorter colon length (p<0.0001, figure 3E,F). H&E staining assay of colon tissues showed that in comparison to the DSS group, the combination treatment resulted in worsening of inflammatory signs, including more infiltrations of inflammatory cells, worsening ulceration, and larger damage to goblet cells (figure 3G).

To validate our previous findings that IL-23 augmented in patients with severe irAEs compared with those without (figure 1B), we further examined the four pro-inflammatory cytokines concentrations in serum from
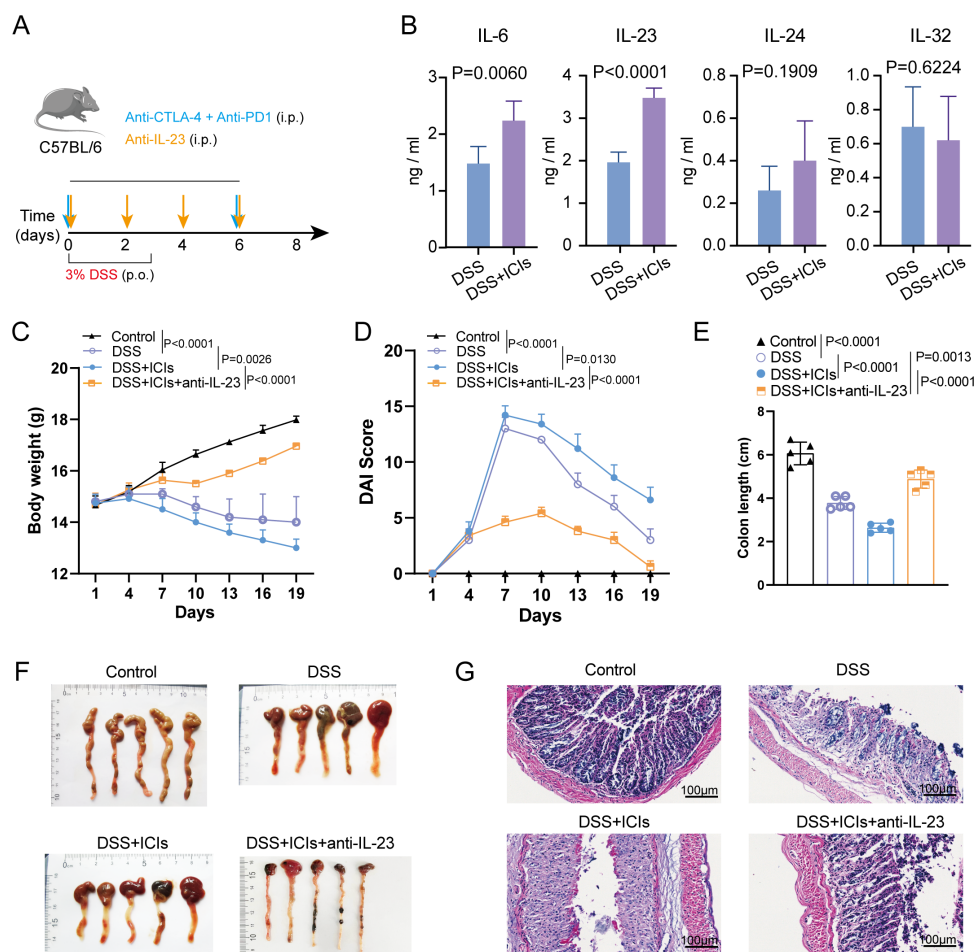


**Figure 3** Combined CTLA-4 and PD-1 blockade exacerbated colitis severity induced by DSS in mice. (A) Mice with DSS-induced colitis were treated intraperitoneally (i.p.) with anti-PD-1 and anti-CTLA-4 monoclonal antibodies, either in combination with IL-23 blockade (using anti-mouse IL-23 antibodies) or without IL-23 blockade. (B) Pro-inflammatory cytokines (IL-6, IL-23, IL-24 and IL-32) concentrations in the serum of mice were analyzed by ELISA analysis. (C) Relative body weight changes throughout the experiment. (D) Evaluation of Disease Activity Index (DAI) during the experiment. Quantitative length (E) and representative images (f) of the colon in mice receiving various treatments. (G) H&E-staining assay of mice colon. CTLA-4, cytotoxic T-lymphocyte associated protein antigen 4; DSS, dextran sulfate sodium salt; ICI, immune checkpoint inhibitor; IL, interleukin; PD-1, programmed cell death protein-1; p.o. , per os.

mice with or without a combination of anti-CTLA-4 and anti-PD-1 monoclonal antibodies treatment. Consistent with our previous findings, the combination treatment induced increased IL-6 (p=0.0061, figure 3B) and IL-23 (p<0.0001, figure 3B) production, while IL-24 (p=0.1909, figure 3B) and IL-32 (p=0.6224, figure 3B) had no significantly. Moreover, IL-23 showed a more significant increase than IL-6, suggesting that increased IL-23 expression might be a vital factor causing the exacerbating colitis.

IL-23 blockade with risankizumab, an IL-23 monoclonal antibody, is recommended for cases that are suffering autoimmune colitis.[13] Therefore, given the above, we further investigated the effect of prophylactic administration of IL-23 on colitis exacerbated by dual anti-CTLA-4 and anti-PD-1 treatment. Surprisingly, we found that prophylactic administration of the monoclonal antibody anti-mouse IL-23 clearly ameliorated the treatment-induced worsening of DSS-induced colitis, including increased body weight (p<0.0001, figure 3C), decreased DAI score (p<0.0001, figure 3D), longer colon length (p<0.0001, figure 3E,F) and improvement of inflammatory signs (figure 3G).

### Prophylactic IL-23 blockade effectively reduces irAEs incidence

In order to prove the robustness of the relationship between IL-23 and irAEs, we further constructed a new irAEs murine model by only adopting the treatment scheme of anti-PD-1 and anti-CTLA-4 combined administration twice a week for 3 weeks (figure 4A). Each group contained 10 mice. IrAEs incidence in mice treated with or without IL-23 blockade was evaluated. We found that 6 of 10 mice (60%) treated with anti-PD-1 and anti-CTLA-4 combined administration in ICIs group exhibited irAEs (figure 4B), including hepatitis (ALT: p=0.0080; AST: p=0.0076, figure 4D; figure 4E), myocarditis (figure 4E), lung inflammation (figure 4E), splenitis (figure 4E) and colitis (figure 4E,H and I). Surprisingly, we also found that mice with irAEs showed higher protein levels of IL-23 at baseline compared with those without irAEs in ICIs group (p=0.0006, figure 4C), which was consistent with our previous findings derived from retrospective analysis based on the GSE186143 data set.

Notably, all 10 mice (100%) treated with prophylactic IL-23 blockade in the ICIs+anti-IL-23 group successfully avoided irAEs (figure 4B). Specifically, IL-23 blockade significantly decreased levels of ALT (p=0.0086, figure 4D) and AST (p=0.0078, figure 4D) in blood, lengthened colon (p<0.0001, figure 4H,I), improved inflammatory pathological features in liver, heart, lung, spleen and colon (figure 4E), and reduced levels of CD11b$^+$Ly6G$^+$ neutrophils in the lung (p=0.0007, figure 4F), spleen (p=0.0003, figure 4G) and colon (p=0.0141, figure 4J).

### Prophylactic IL-23 blockade does not hinder the antitumor activity of combined anti-PD-1 and anti-CTLA-4 immunotherapy

To determine whether the ameliorating effects of colitis induced by dual anti-PD-1 and anti-CTLA-4 treatment would also occur in B16-BL6 tumor-bearing mice in which colitis had been concomitantly induced by DSS, engraft tumor model was successfully established, refer to the method of previous research[9] (figure 5A). Treating these mice with combined anti-PD-1 and anti-CTLA-4 exacerbated the DSS-induced colitis and resulted in reduced body weight (p<0.0001, figure 5B), increased DAI score (p=0.0240, figure 5C), shorter colon length (p=0.0141, figure 5D) and worsening of colon inflammation (figure 5E). Treating mice with anti-mouse IL-23 antibody concomitantly with combined CTLA-4 and PD-1 immunotherapy markedly ameliorates autoimmune colitis, which was characterized by increased body weight (p<0.0001, figure 5B), decreased DAI score (p<0.0001, figure 5C), longer colon length (p=0.0001, figure 5D) and improvement of inflammatory signs (figure 5E).

We next sought to determine whether prophylactic IL-23 blockade would affect the antitumor activity of the anti-PD-1 and anti-CTLA-4 combination in mice with established B16-BL6-derived tumors. We found that the tumor volume (p=0.8251, figure 5F,G) and survival time (p=0.5651, figure 5H) of mice simultaneously received anti-mouse IL-23 antibody and combined CTLA-4 and PD-1 immunotherapy were not significantly different from those received combined CTLA-4 and PD-1 immunotherapy alone.

These data indicated that prophylactic blockade of IL-23 improved colitis in mice with B16-BL6-derived tumors, but did not impair the antitumor effects of anti-PD-1 and anti-CTLA-4 combination.

### IL-23 blockade decreased the infiltration of CD4$^+$ Tems in spleens and B16-BL6 -derived tumors from mice

In our retrospective analysis, we found that augmented CD4$^+$ Tems, broadly reflected in peripheral blood samples, might preferentially underlie irAEs onset (figure 2L). Therefore, to investigate whether the improved colitis effects of prophylactic IL-23 blockade could be related to the reversion of an exhaustion phenotype of CD4$^+$ Tems, we further examined immune cells concentrations in spleens and tumors using flow cytometry analysis (online supplemental figure S5A). We observed an increase of spleen-infiltrating or tumor-infiltrating CD4$^+$ Tems in mice with ICIs-related intestinal toxicity after receiving DSS+ICIs treatment (spleen: online supplemental figure S5B, p=0.0017; tumor: online supplemental figure S5G, p<0.0001), which was restrained by prophylactic IL-23 blockade therapy (spleen: online supplemental figure S5B, p=0.0005; tumor: online supplemental figure S5G, p<0.0001). However, we did not detect any changes in CD8$^+$ T (online supplemental figure S5C,H), natural killer (NK) (online supplemental figure S5D,I), dendritic cell (DC) (online supplemental figure S5E,J)
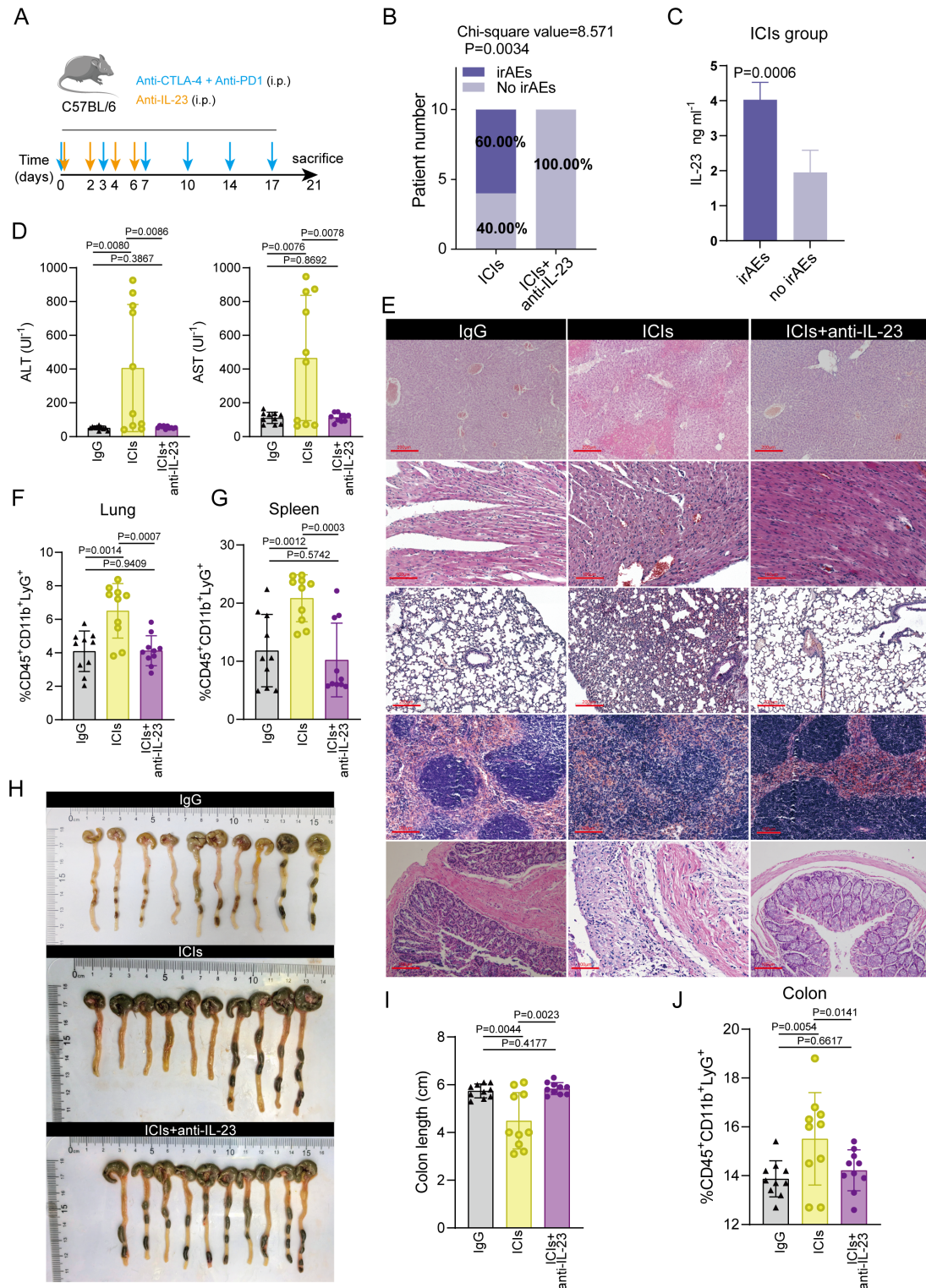
**Figure 4** IL-23 blockade can protect mice from irAEs. (A) Schematic representation of the treatments applied to C57/BL6 mice that were treated intraperitoneally (i.p.) with 200 µg anti-mouse PD-1 (InVivoMAb Bio X Cell; anti-mouse PD-1, clone RMP1-14) and 150 µg anti-mouse CTLA-4 (InVivoMAb Bio X Cell; anti-mouse CTLA-4, clone 9D9) or the IgG isotype twice a week for 3 weeks, either in combination with 100 ng anti-mouse IL-23 (clone G23-8, No. 14–7232; eBioscience) or without on days 0, 2, 4 and 6. The mice were sacrificed for analysis on day 21 after the first treatment. (B) The irAEs incidence of mice in ICIs group and in ICIs+anti-IL-23 group. (C) The protein level of IL-23 at baseline in the serum of mice with or without irAEs in ICIs group. (D) The levels of alanine transaminase (ALT) and aspartate transaminase (AST) in serum on day 21. (E) H&E-staining assay of liver, heart, lung, spleen and colon tissues. CD11b+Ly6G+ neutrophils of the lung (F) and spleen (G) were analyzed by flow cytometry. Representative images (H) and quantitative length (I) of the colon in mice receiving various treatments. (J) CD11b+Ly6G+ neutrophils of the colon were analyzed by flow cytometry. CTLA-4, cytotoxic T-lymphocyte associated protein 4; ICI, immune checkpoint inhibitor; IL, interleukin; irAE, immune-related adverse event; PD-1, programmed cell death protein-1.
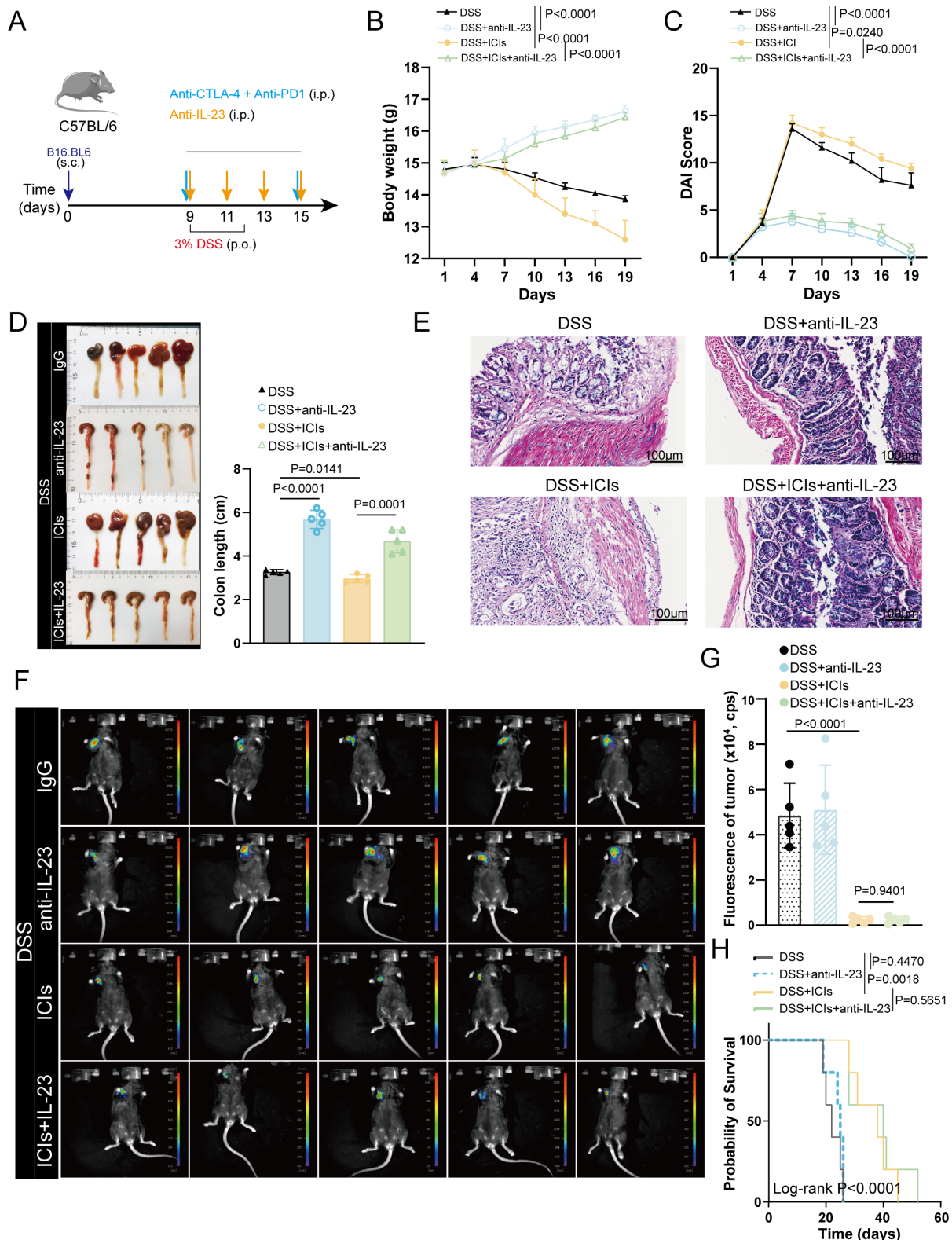
**Figure 5** Prophylactic IL-23 blockade ameliorated DSS-induced colitis exacerbated by anti-PD-1 and anti-CTLA-4 therapy in mice with B16.BL6-derived tumors. (A) Schematic representation of the treatments applied to mice that were subcutaneously (s.c.) engrafted with B16.BL6 mouse melanoma cells. Simultaneously, mice were induced colitis from day 9 by providing DSS in the drinking water. (B) Relative body weight changes throughout the experiment. (C) Evaluation of Disease Activity Index (DAI) during the experiment. (D) Change of colon length during the experiment. (E) H&E-staining assay of mice colon. (F) Small animal imaging showed the fluorescence of tumors in the xenograft mice of each group (n=5). (G) Quantification of B16.BL6-derived tumors in four groups of mice. (H) Kaplan-Meier survival curves of mice. CTLA-4, cytotoxic T-lymphocyte associated protein antigen 4; DSS, dextran sulfate sodium salt; ICI, immune checkpoint inhibitor; IL, interleukin; i.p. , intraperitoneally; PD-1, programmed cell death protein-1; p.o. , per os.

and macrophages (online supplemental figure S5F,K) cell proportions in spleens and tumors between mice in DSS+ICIs groups and DSS+ICIs+anti-IL-23 groups.

Moreover, we also found that mice in DSS+ICIs group strongly elevated CD8$^+$ Tems (spleen: online supplemental figure S5C, p<0.0001; tumor: online supplemental figure S5H, p=0.0022), NK cells (spleen: online supplemental figure S5D, p<0.0001; tumor: online supplemental figure S5I, p=0.0014), M1 macrophages (spleen: online supplemental figure S5F, p=0.0211; tumor: online supplemental figure S5K, p<0.0001) frequency in spleens and tumors compared with mice in DSS group. However, there was no significant difference in CD8$^+$ Tcms (online supplemental figure S5C,H), DC cells (online supplemental figure S5E,J), M2 macrophages (online supplemental figure S5F,K) infiltrating proportions in spleens and tumors between mice in DSS groups and DSS+ICIs groups.

Collectively, these findings indicate that augmented CD4$^+$ Tems may preferentially underlie irAEs onset, which can be restrained by prophylactic IL-23 blockade therapy.

### IL-23 is involved in immune checkpoint blockade-induced toxicity in a humanized mouse model

To further explore the applicability of our findings, we used a xenograft-versus-host model of disease, in which human PBMCs were infused into Rag2$^{-/-}$Il2rg$^{-/-}$ mice. This condition causes the inflammation of several target organs, including the colon.[33] Therefore, referring to methods as previous researcher reported,[9] we created a model in which Rag2$^{-/-}$Il2rg$^{-/-}$ mice were adoptively transferred with PBMCs, causing graft-versus-host disease that was further exacerbated by dual anti-PD-1 and anti-CTLA-4 treatment (figure 6A). Treating these mice with combined anti-PD-1 and anti-CTLA-4 treatment resulted in hepatitis (ALT: p=0.0145; AST: p=0.0022, figure 6B), colitis (figure 6C,D) and lung inflammation (figure 6F). In addition, neutrophils have been proven to be involved in the effector phase of irAEs development.[34] Therefore, we also analyzed levels of CD11b$^+$Ly6G$^+$ neutrophils in mice and found a strong increase, compared with control-treated mice, in both colon (p<0.0001, figure 6E) and lung tissues (p<0.0001, figure 6G) of ICIs-treated mice, which are major irAEs target organs.

Notably, prophylactic IL-23 blockade with risankizumab significantly reduced irAEs severity in the major irAEs target organs, including the liver, colon, and lung. Specifically, treating mice with IL-23 inhibitors concomitantly with combined CTLA-4 and PD-1 immunotherapy markedly decreased levels of ALT (p=0.0145, figure 6B) and AST (p=0.0019, figure 6B) in blood, longer colon length (p<0.0001, figure 6C), improvement of inflammatory signs in colon and lung (figure 6D,F) and reduced levels of CD11b$^+$Ly6G$^+$ neutrophils in both the colon (p<0.0001, figure 6E) and the lung (p<0.0001, figure 6G).

To determine whether prophylactic IL-23 blockade would affect the antitumor activity of the anti-PD-1 and anti-CTLA-4 combination against A375-derived tumors in our humanized mouse model, we further compare the tumor volume and survival time of mice among three groups. We observed that tumor progression was controlled to some extent by dual CTLA-4 and PD-1 immunotherapy (figure 6H–J). Moreover, concomitant IL-23 blockade treatment did not diminish these therapeutic effects (figure 6H–J).

To further explore the feasibility of IL-23 as a biomarker in the clinic, we further collected blood samples from patients with colitis and healthy individuals to test protein levels of IL-23 in serum. 10 patients with colitis and 10 healthy individuals were included in this analysis. ELISA test indicated that the protein level of IL-23 in patients with colitis was significantly higher than that in healthy individuals (online supplemental figure S6). Specifically, the average protein level of IL-23 in the serum of patients with colitis was 82.28±0.54 pg/mL, whereas the average expression level of IL-23 in the serum of healthy individuals was 36.26±1.23 pg/mL. These results confirmed that the levels of IL-23 protein in serum can be used as a biomarker for clinical detection.

### The blood-based composite model has predictive potential for severe irAEs, ICIs response and autoimmune disease

Given these results, we wondered whether a composite model integrating both features—IL-23 and CD4$^+$ T-cell abundance—might outperform either feature alone for severe irAEs. We first use a logistic regression framework to train a composite model using CD4$^+$ T-cell types identified with top three predictive power for severe irAEs in previous findings (figure 7A). CD4$^+$ T cell (EPIC) combined with IL-23 was found to achieve superior performance for predicting severe irAEs (training cohort: AUC=0.843; testing cohort: AUC=0.807; all patients: AUC=0.832, figure 7B,C). Thus, the composite model, consisting of CD4$^+$ T cell (EPIC) and IL-23, were involved in our next analysis. We observed that the composite model could well discriminate severe from non-severe irAEs patients, indicating the strong potential of the model for predicting the future development of severe irAEs (figure 7D,E). Patients who developed severe irAEs tended to have increased composite model score, compared with those who did not (figure 7F). In reverse, patients in the high composite model score group demonstrated marked severe irAEs incidence compared with those in the low score group (figure 7G). Moreover, the composite model score was progressively increased in the grade of severe irAEs, and ascended to the highest levels in grade 4 (figure 7H,I).

To test whether the pretreatment composite model could predict time-to-severe irAEs, we next assigned patients to high versus low groups by median score value as the cut-off value in train, test or all cohort, respectively. In train cohort, patients in the high group experienced severe irAEs after treatment initiation, whereas the vast majority of patients in the low group little experienced severe irAEs (train cohort: p=0.0295, figure 7J). Similar results were seen in the test (test cohort: p=0.0134, figure 7J) or all cohorts (all cohort: p<0.0001, figure 7J).
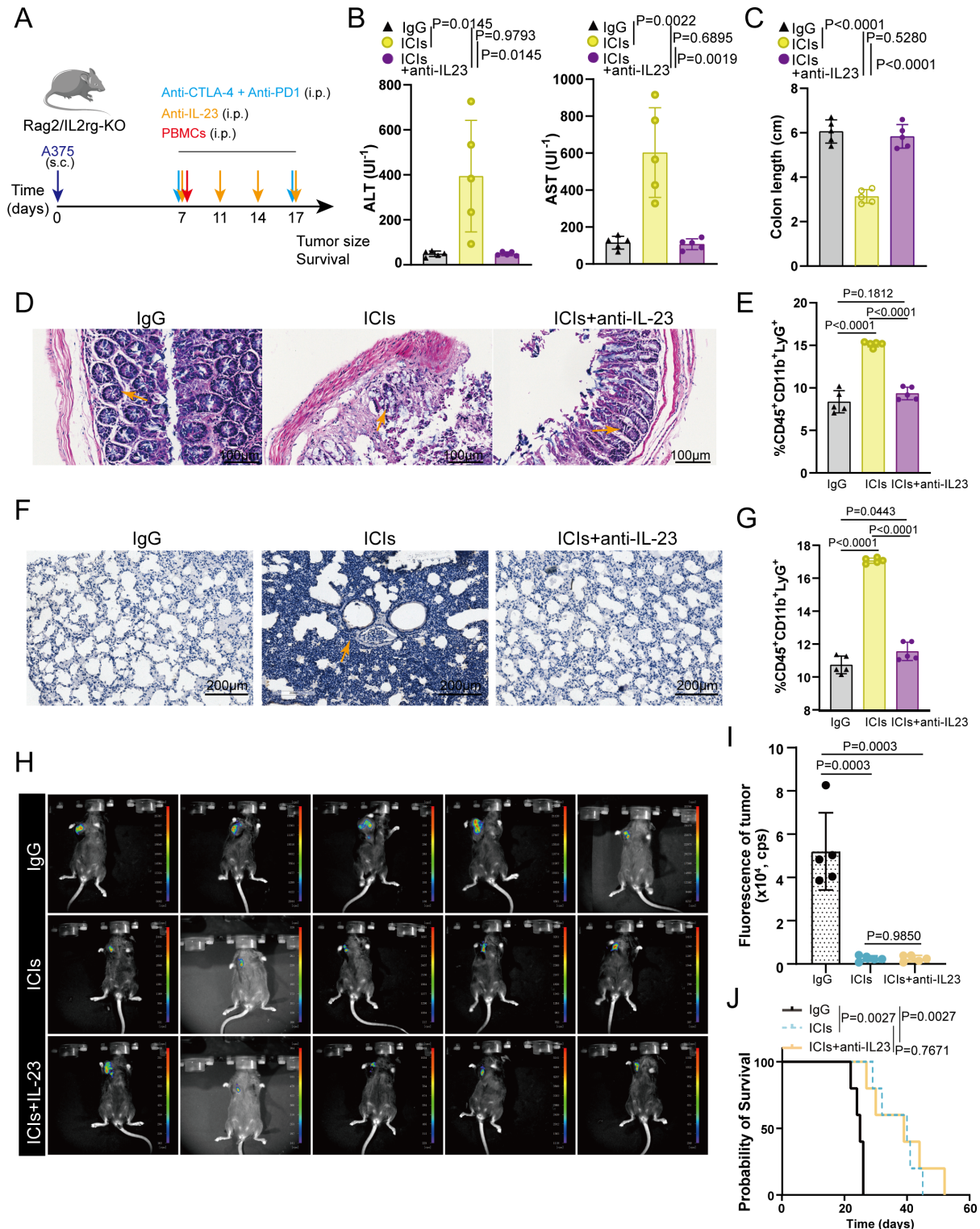
**Figure 6** IL-23 was involved in immune checkpoint blockade induced in a humanized mouse model. (A) Schematic representation of the treatments applied to immunodeficient Rag2$^{-/-}$Il2rg$^{-/-}$ mice that were first subcutaneously engrafted with A375 human melanoma cells, followed by the infusion of human PBMCs after 7 days. Mice were injected on days 7, 11, 14 and 17 intraperitoneally with combined anti-PD-1 and anti-CTLA-4 therapy, with or without risankizumab. As an antibody control, we used human polyclonal IgG. (B) The levels of alanine transaminase (ALT) and aspartate transaminase (AST) in serum on day 21. (C) Quantitation of colon length in mice receiving various treatments. H&E-staining assay of the colon (D) and lung (F) tissues. Colon and lung were isolated and digested on day 21. CD11b$^+$Ly6G$^+$ neutrophils of the colon (E) and lung (G) were analyzed by flow cytometry. (H) Small animal imaging showed the fluorescence of tumors in the xenograft mice of each group (n=5). (I) Quantificational fluorescence of B16.BL6-derived tumors in four groups of mice. (J) Kaplan-Meier survival curves of mice. CTLA-4, cytotoxic T-lymphocyte associated protein 4; ICI, immune checkpoint inhibitor; IL, interleukin; i.p., intraperitoneally; PBMC, peripheral blood mononuclear cell; PD-1, programmed cell death protein-1; s.c., subcutaneously.
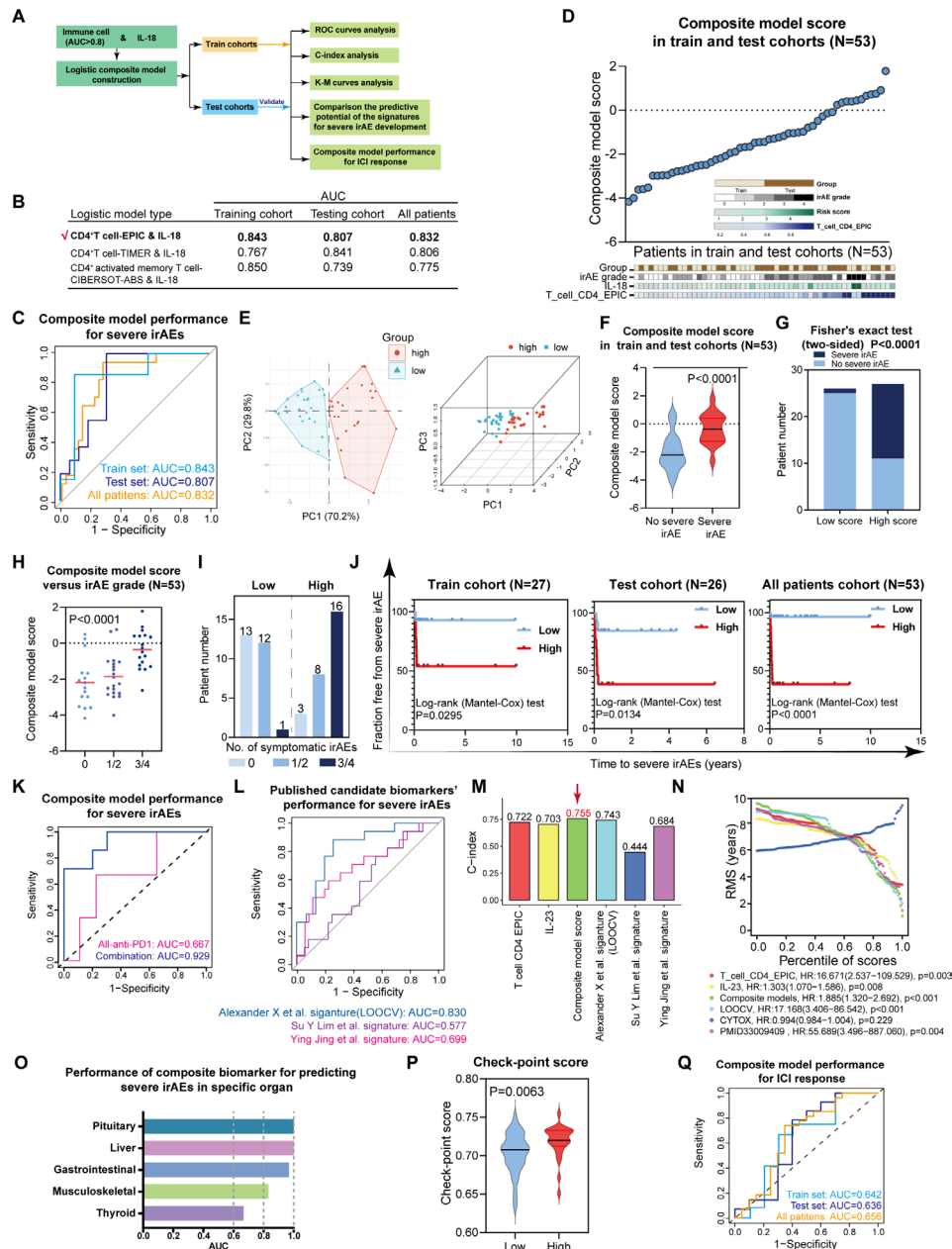
**Figure 7** Composite model performance for predicting severe irAEs and ICIs response across irAEs grade and ICIs regiments. (A) The strategy of constructing a composite model to predict severe irAEs. (B) Comparison of AUCs calculated using three composite models for severe irAEs in GSE186143. (C) ROC plots showed the composite model performance in train, test and all patients sets. (D) Development of a composite model for the prediction of severe irAEs, integrating CD4$^+$ T-cell abundance and IL-23 from pretreatment peripheral blood transcriptomes, with model scores trained on train set and shown across all patients. (E) Principal components analysis of the scores between low-risk and high-risk samples stratified by the composition model in melanoma. (F) The difference of the composite model scores between severe and no severe irAEs subgroups. (G) Fraction of patients with low scores versus those with high scores, stratified by the composite model. Significance was determined by a two-sided Fisher's exact test. (H) Composite model scores across patients with various grades of irAEs. (I) Number of patients in various grades of irAEs. (J) Kaplan-Meier analysis for freedom from severe irAEs in train cohort (left), test cohort (middle) and all patients cohort (right), stratified by the composite model scores. (K) ROC plot showing composite model performance in patients with melanoma, whether applied to combination therapy patients or programmed cell death protein-1 monotherapy patients. The AUC is shown for each ROC curve. (L) Published candidate biomarkers' performance for severe irAEs in all patients. (M) The C-index scores for severe irAEs prediction of our composite model score, single features and published candidate biomarkers. (N) RMS of our composite model score, single features and published candidate biomarkers. (O) Performance of composite model for specific organ adverse effects based on GSE186143 data set, which assessed by receiver operating characteristic (ROC) analysis. (P) The difference of the check-point genes expression between low-risk and high-risk subgroups stratified by the composite model. (Q) The composite model performance for ICIs response in train, test and all patient cohorts. AUC, area under the curve; ICI, immune checkpoint inhibitor; IL, interleukin; irAE, immune-related adverse event; K-M, Kaplan-Meier; RMS, recession modeling strategy.

Moreover, the composite model maintained predictive potential for severe irAEs prediction in each therapy type group separately, whether assessed in the combination therapy cohort (AUC: 0.929, figure 7K) or anti-PD-1 cohort (AUC: 0.667, figure 7K).

To test the predictive performance of the composite model, we next evaluated the AUC value and C-index score of the composite model and some previously published candidate biomarkers[12 15 16] assessed in bulk transcriptomic data. Indeed, the AUC values of all published candidate biomarkers were less than the AUC values of the composite model (figure 7C,L). In addition, the composite model observed the highest concordance index (C-index) score of 0.755, outperforming either feature alone or published (figure 7M,N). Given the above, the composite model integrating both features—IL-23 and CD4$^+$ T-cell abundance—might outperform either feature alone or published for severe irAEs.

To explore the composite biomarker performance for predicting irAEs in specific organ system, patients with complete information on irAEs-related organs were further involved in this analysis based on the GSE186143 data set. Composite model scores were assessed by ROC analysis. Models trained to discriminate severe from non-severe irAEs were used to predict the future development of severe irAEs. The results showed that the pretreatment composite model was also effective for specific organ adverse effects, including pituitary (AUC=1.00, figure 7O, online supplemental figure S7A), liver (AUC=1.00, figure 7O, online supplemental figure S7B), gastrointestinal (AUC=0.969, figure 7O, online supplemental figure S7C), musculoskeletal adverse events (AUC=0.833, figure 7O, online supplemental figure S7D), although with reduced performance for thyroid adverse events (AUC=0.667, figure 7O, online supplemental figure S7E). These findings indicated that regardless of irAEs-affected organ system, the pretreatment composite model remained predictive for severe irAEs.

Given that irAEs onset appears to be significantly associated with ICIs response, we wondered whether the composite model could also predict ICIs response. Indeed, in the high score group, the expression of checkpoint genes were found to be significantly increased, compared with the low score group (p=0.0063, figure 7P). Moreover, the composite model yielded an AUC of 0.642 in train cohort, an AUC of 0.636 in test cohort and an AUC of 0.656 in all cohorts (figure 7Q), indicating its moderately predictive potential for ICIs response.

Moreover, compared with healthy controls, the score of the composite model was also markedly augmented in patients with IBD (p<0.0001, online supplemental figure S8A) and SLE (p=0.0003, online supplemental figure S8C). The composite model was yielded an AUC of 0.707 in the IBD-GSE100833 data set (online supplemental figure S8B) and an AUC of 0.756 in the SLE-GSE72509 data set (online supplemental figure S8D), indicating its persistently moderate potential for autoimmunity prediction.

These data indicated the composite model consists of two novel blood-based features—IL-23 and CD4$^+$ Tems—that may have predictive potential for severe irAEs, ICIs response and autoimmune disease, underscoring its diversification of applications.

## DISCUSSION

Up to 60% of patients with cancer treated with ICIs experience severe irAEs, which involve inflammation in healthy tissues and can manifest as rashes, arthritis, endocrinopathies, enteropathy, and pneumonitis.[6 7] Clearly, irAEs pose a significant obstacle in the creation of a diverse multiagent immunotherapy plan that is necessary to combat the heterogenous and treatment-resistant tumor microenvironment.[35] Early recognition and intervention are critical for severe irAEs, which has fueled intensive efforts to unveil what drives the irAEs, which is not only relevant for ICIs implementation, but also provides therapeutic strategies to treat irAEs better. Hence, this study involved extensive examination of irAEs immunobiology through clinical, translational, and preclinical analyses.

Here we find that (1) IL-23 markedly elevates in patients with severe irAEs compared with those with no severe irAEs through retrospective analysis and in vivo analysis using mice model with irAEs; (2) treating mice with anti-mouse IL-23 antibody concomitantly with combined CTLA-4 and PD-1 immunotherapy ameliorates colitis and, in addition, preserves antitumor efficacy; (3) murine models with graft-versus-host disease was established, in which Rag2$^{-/-}$Il2rg$^{-/-}$ mice were transferred with human PBMCs and received combined CTLA-4 and PD-1 treatment. When human melanoma cells were xenografted into these mice, prophylactic blockade of human IL-23 using clinically available IL-23 inhibitor (risankizumab) ameliorated colitis, hepatitis and lung inflammation in xenografted mice, and moreover, immunotherapeutic control of xenografted tumors was retained; (4) augmented CD4$^+$ Tems, broadly reflected in bulk transcriptome, single-cell profiles from peripheral blood and mice model with ICIs-induced irAEs, may preferentially underlie irAEs onset, and were significantly associated with autoimmune disorders relative to healthy individuals; (5) a machine learning-based computational framework based on two blood-based features—IL-23 and CD4$^+$ Tems—outperforms either feature alone and other published candidate biomarkers[12 15 16] for predicting severe irAEs, and also can predict ICIs response and autoimmune disease.

IL-23, a powerful pro-inflammatory cytokine, plays a role in numerous innate and adaptive immune processes associated with infection, inflammation, and autoimmunity. Hence, it is additionally referred to as a crucial intermediary of auto-inflammatory conditions linked to autoimmune ailments.[36] IL-23 blockade is a recommended treatment for ulcerative colitis and Crohn's disease.[13] A previous research in 2023 found that the response to lymphocytes expressing IFN-γ was

the most significantly activated pathway in the development of ICIs-induced colitis.[37] Then, IL-23 was proved as the upstream mediator responsible for activating IFN-γ expression in ICIs-induced colitis. Preclinical model of ICIs-colitis could be attenuated by IL-23 blockade via reducing the number of IFN-γ producing CD4+ T cells in the colon and especially IFN-γ/TNF-α co-producing cells. This is to some extent consistent with our findings that prophylactic IL-23 blockade restrains CD4+ Tems infiltrations, which may be the potential molecular mechanism by which IL-23 blockade prevents irAEs onset. However, they only demonstrated the therapeutic effect of IL-23 blockade on existing ICIs-induced colitis, and did not explore the preventive effect of prophylactic administration of IL-23 blockage in reducing the incidence and severity of ICIs-induced colitis, and its impact on the efficacy of immunotherapy. Our research fills these gaps, and indicates that prophylactic blockade of IL-23 effectively reduces irAEs incidence through ameliorating hepatitis, colitis, splenitis and lung inflammation induced by dual CTLA-4 and PD-1 immunotherapy, and moreover, does not impair the antitumor effects, which provides clinically feasible strategies to dissociate efficacy and toxicity in the use of combined ICIs for cancer immunotherapy. Moreover, a clinical case report also proved that IL-12/23 blockade showed a therapeutic effect for refractory ICIs-induced colitis.[38] Although they only demonstrated the therapeutic effect of IL-23 blockade on existing ICIs-induced colitis and did not prove the preventive effect of IL-23 blockade in reducing colitis incidence, they also provided clinical data support for the future application of prophylactic IL-23 blockade as a new therapeutic regimen to prevent irAEs onset in patients with cancer.

Previous study indicated that IL-23 is primarily produced by cells of the mononuclear phagocyte system.[39] In a recent research, Tobias Wertheimer et al found tumor-associated macrophages to be the main source of IL-23 in mouse and human tumor microenvironments.[40] Consistent with previous studies, in this work, we found that IL-23, as a severe-irAEs-associated gene, was mainly transcribed by monocytes in human peripheral blood based on scRNA-seq analysis.

To validate our findings in tumor-bearing mouse models with autoimmune diseases, murine models with graft-versus-host disease were established, in which Rag2$^{-/-}$Il2rg$^{-/-}$ mice were transferred with human PBMCs and received combined CTLA-4 and PD-1 treatment. When human melanoma cells were xenografted into these mice, combined CTLA-4 and PD-1 immunotherapy in mice with B16 tumors led to an increase in CD8+ and CD4+ Tems, M1 macrophages and NK cells in the tumor infiltrate, and this was appeased by anti-IL-23 treatment. Notably, prophylactic blockade of human IL-23 ameliorated colitis and hepatitis in xenografted mice, and moreover, immunotherapeutic control of xenografted tumors was retained.

Following treatment with ICIs for melanoma, approximately 25% of patients developed novel autoantibodies. Several studies have shown that individuals with autoimmunity who received ICIs were prone to experiencing exacerbations in their autoimmune symptoms.[10 11] In this work, we found that effective memory CD4+ T cells were significantly associated with autoimmune disorders relative to healthy individuals, paralleling the immune landscape of severe irAEs development. These data suggest that elevated effective memory CD4+ T cells, as a common immunological feature underlying both irAEs development and autoimmune disease, are significantly enriched in autoimmune disorders relative to healthy individuals, such as SLE and IBD, which needs further validation in future experiment studies.

Early diversification of the circulating T-cell repertoire, as a prime factor, has been related to both response and ICIs toxicity.[1 41] Specifically, T cells have been found in synovium during ICI-induced arthritis[42] and the thyroid during ICIs-induced thyroiditis.[43] Therefore, evaluating immunological features is in extremely urgent to understand what drives the irAEs, providing therapeutic strategies to better treat autoimmune disorders. In this paper, we further set out to systematically evaluate immunological features associated with ICIs-induced toxicity in patients with melanoma, and observed that CD4+ T cells strongly link to severe irAEs development. Additionally, effector memory CD4+ T cell, type 17 helper cell and effector memory CD8+ T cell were the top three categories that were most significantly elevated in patients who experienced irAEs. Particularly, effector memory CD4+ T cell showed the strongest association with irAEs among these T cells. Lozano et al discovered that the presence of activated memory CD4+ T cells and the diversity of TCR in the peripheral blood before ICIs treatment were linked to the occurrence of severe irAE.[12] These findings are consistent with our findings that effector memory CD4+ T-cell links to severe irAEs onset.

Key questions regarding the complete nature of the relationship between irAEs and ICIs response remain unsettled. The most pertinent of these involve whether irAEs severity and therapeutic regimen are related to ICIs effectiveness.[27] Previous research indicated that patients who experience more severe irAEs should have increased T-cell activity and experience better outcomes compared with those who experience lower-grade irAEs.[44] In contrast, Henry Quach et al demonstrated that there was no relationship between irAEs severity and ICIs efficacy.[45] In our study, our findings supported the standpoint that the severity of irAEs was not associated with the ICIs response rate, which provided further evidence support to address the key problem of the controversial relationship between irAEs and ICIs response. As for therapeutic regimen, patients who experience irAEs while on therapy with anti-PD-1 and anti-programmed death-ligand 1 antibodies have been documented to experience improved outcomes,[46] but in patients treated with anti-CTLA-4 antibodies, this association has been less uniform.[47] In this

work, we found that the ICIs response rate of patients with irAEs who received anti-PD-1 treatment was higher than that of patients without irAEs, but in patients who received combination anti-PD-1 and anti-CTLA-4 antibodies therapy, irAEs onset displayed no significant correlation with ICIs response rate. These findings filled the gap in the previous evidence that there was no correlation between irAEs and ICIs response in patients treated with anti-CTLA-4 therapy.

There are inevitably several limitations of our study that should be acknowledged. First, it is yet to be determined if our findings apply to late-onset irAEs, as the development of severe irAEs occurred within a period of less than 3 months in our cohorts. Second, it is yet unclear whether our composite model will persistently apply to predict ICIs-related irAEs development in other cancer types, except for melanoma. Third, we also recognize that IL-23/CD4$^+$ Tems are not the only pathway, but other cytokines may be involved. For example, in a study conducted by Yifan Zhou and his teams, it was discovered that colonic neutrophil accumulation and systemic IL-6 release were caused by αCTLA-4–mediated irAEs.[48] Finally, another limitation is the lack of good murine models for ICIs-induced irAEs. It is expected that mouse with irAEs models developed in the future that more closely resemble human conditions will be developed for further validation experiments.

## CONCLUSION

Our results indicate that an anti-IL-23 agent may—at least in the lung, gut and liver—improve the safety of dual anti-CTLA-4 and anti-PD-1 treatment, and moreover, immunotherapeutic control of tumors was retained. In addition, we also develop a composite model based on two blood-based features—IL-23 and CD4$^+$ Tems—that may have predictive potential for severe irAEs, ICIs response and autoimmune disease, underscoring its diversification of applications. This study not only provides a new strategy for the prevention or treatment of irAEs, but also provides a reliable potential biomarker for early prediction of irAEs onset.

**Author affiliations**
$^1$Department of Pharmacology, School of Pharmacy, China Medical University, Shenyang, China
$^2$Liaoning Key Laboratory of molecular targeted anti-tumor drug development and evaluation; Liaoning Cancer immune peptide drug Engineering Technology Research Center; Key Laboratory of Precision Diagnosis and Treatment of Gastrointestinal Tumors, Ministry of Education, China Medical University, Shenyang, China
$^3$Liaoning Medical Diagnosis and Treatment Center, Shenyang, China
$^4$Department of Radiation Oncology, The First Affiliated Hospital of China Medical University, Shenyang, China
$^5$Department of Orthopedics, Shengjing Hospital of China Medical University, Shenyang, China

**ORCID iDs**
Mingyi Ju http://orcid.org/0000-0002-4084-3358
Lianghua Ma http://orcid.org/0000-0003-0116-0869

## REFERENCES

1 Morad G, Helmink BA, Sharma P, *et al*. Hallmarks of response, resistance, and toxicity to immune checkpoint blockade. *Cell* 2021;184:5309–37.
2 Pauken KE, Dougan M, Rose NR, *et al*. Adverse events following cancer immunotherapy: obstacles and opportunities. *Trends Immunol* 2019;40:511–23.
3 Postow MA, Sidlow R, Hellmann MD. Immune-related adverse events associated with immune checkpoint blockade. *N Engl J Med* 2018;378:158–68.
4 Suarez-Almazor ME, Kim ST, Abdel-Wahab N, *et al*. Review: immune-related adverse events with use of checkpoint inhibitors for immunotherapy of cancer. *Arthritis Rheumatol* 2017;69:687–99.
5 Blum SM, Rouhani SJ, Sullivan RJ. Effects of immune-related adverse events (irAEs) and their treatment on antitumor immune responses. *Immunol Rev* 2023;318:167–78.
6 Smithy JW, Faleck DM, Postow MA. Facts and hopes in prediction, diagnosis, and treatment of immune-related adverse events. *Clin Cancer Res* 2022;28:1250–7.
7 Hodi FS, Chiarion-Sileni V, Gonzalez R, *et al*. Nivolumab plus ipilimumab or nivolumab alone versus ipilimumab alone in advanced melanoma (CheckMate 067): 4-year outcomes of a multicentre, randomised, phase 3 trial. *Lancet Oncol* 2018;19:1480–92.
8 Hailemichael Y, Johnson DH, Abdel-Wahab N, *et al*. Interleukin-6 blockade abrogates immunotherapy toxicity and promotes tumor immunity. *Cancer Cell* 2022;40:509–23.
9 Perez-Ruiz E, Minute L, Otano I, *et al*. Prophylactic TNF blockade uncouples efficacy and toxicity in dual CTLA-4 and PD-1 immunotherapy. *Nature New Biol* 2019;569:428–32.
10 Johnson DB, Sullivan RJ, Ott PA, *et al*. Ipilimumab therapy in patients with advanced melanoma and preexisting autoimmune disorders. *JAMA Oncol* 2016;2:234–40.
11 Menzies AM, Johnson DB, Ramanujam S, *et al*. Anti-PD-1 therapy in patients with advanced melanoma and preexisting autoimmune disorders or major toxicity with ipilimumab. *Ann Oncol* 2017;28:368–76.

12 Lozano AX, Chaudhuri AA, Nene A, *et al*. T cell characteristics associated with toxicity to immune checkpoint blockade in patients with melanoma. *Nat Med* 2022;28:353–62.

13 Ferrante M, Irving PM, Abreu MT, *et al*. Maintenance risankizumab sustains induction response in patients with Crohn's disease in a randomized phase 3 trial. *J Crohn's Colitis* 2024;18:416–23.

14 Gargiulo L, Ibba L, Valenti M, *et al*. Pembrolizumab-induced plaque psoriasis successfully treated with risankizumab in a patient with stage IV cutaneous melanoma. *Melanoma Res* 2023;33:152–4.

15 Lim SY, Lee JH, Gide TN, *et al*. Circulating cytokines predict immune-related toxicity in melanoma patients receiving anti-PD-1-based immunotherapy. *Clin Cancer Res* 2019;25:1557–63.

16 Jing Y, Liu J, Ye Y, *et al*. Multi-omics prediction of immune-related adverse events during checkpoint immunotherapy. *Nat Commun* 2020;11:4946.

17 Gao X, Fan W, Tan L, *et al*. Soy isoflavones ameliorate experimental colitis by targeting ERα/NLRP3 inflammasome pathways. *J Nutr Biochem* 2020;83:108438.

18 Tsukamoto H, Komohara Y, Tomita Y, *et al*. Aging-associated and CD4 T-cell–dependent ectopic CXCL13 activation predisposes to anti–PD-1 therapy-induced adverse events. *Proc Natl Acad Sci USA* 2022;119:e2205378119.

19 Li T, Fu J, Zeng Z, *et al*. TIMER2.0 for analysis of tumor-infiltrating immune cells. *Nucleic Acids Res* 2020;48:W509–14.

20 Newman AM, Liu CL, Green MR, *et al*. Robust enumeration of cell subsets from tissue expression profiles. *Nat Methods* 2015;12:453–7.

21 Finotello F, Mayer C, Plattner C, *et al*. Molecular and pharmacological modulators of the tumor immune contexture revealed by deconvolution of RNA-seq data. *Genome Med* 2019;11:34.

22 Aran D, Hu Z, Butte AJ. xCell: digitally portraying the tissue cellular heterogeneity landscape. *Genome Biol* 2017;18:220.

23 Becht E, Giraldo NA, Lacroix L, *et al*. Estimating thepopulation abundance of tissue-infiltrating immune and stromal cell populations using gene expression. *Genome Biol* 2016;17:218.

24 Racle J, de Jonge K, Baumgaertner P, *et al*. Simultaneous enumeration of cancer and immune cell types from bulk tumor gene expression data. *Elife* 2017;6:e26476.

25 Miao Y, Zhang Q, Lei Q, *et al*. ImmuCellAI: a unique method for comprehensive T-cell subsets abundance prediction and its application in cancer immunotherapy. *Adv Sci (Weinh)* 2020;7:1902880.

26 Yoshihara K, Shahmoradgoli M, Martínez E, *et al*. Inferring tumour purity and stromal and immune cell admixture from expression data. *Nat Commun* 2013;4:2612.

27 Das S, Johnson DB. Immune-related adverse events and anti-tumor efficacy of immune checkpoint inhibitors. *J Immunother Cancer* 2019;7:306.

28 Luoma AM, Suo S, Williams HL, *et al*. Molecular pathways of colon inflammation induced by cancer immunotherapy. *Cell* 2020;182:655–71.

29 Subudhi SK, Aparicio A, Gao J, *et al*. Clonal expansion of CD8 T cells in the systemic circulation precedes development of ipilimumab-induced toxicities. *Proc Natl Acad Sci USA* 2016;113:11919–24.

30 Chiffelle J, Genolet R, Perez MA, *et al*. T-cell repertoire analysis and metrics of diversity and clonality. *Curr Opin Biotechnol* 2020;65:284–95.

31 Postow MA, Hellmann MD. Adverse events associated with immune checkpoint blockade. *N Engl J Med* 2018;378:1165.

32 Eichele DD, Kharbanda KK. Dextran sodium sulfate colitis murine model: an indispensable tool for advancing our understanding of inflammatory bowel diseases pathogenesis. *World J Gastroenterol* 2017;23:6016–29.

33 Sanmamed MF, Rodriguez I, Schalper KA, *et al*. Nivolumab and urelumab enhance antitumor activity of human T lymphocytes engrafted in Rag2-/-IL2Rγnull immunodeficient mice. *Cancer Res* 2015;75:3466–78.

34 Hirschhorn D, Ricca J, Gasmi B, *et al*. A delicate interplay between adaptive and innate immunity caused by immunotherapy triggers tumor immunity and aseptic inflammation. *J Immunol* 2018;200:178.

35 Kalbasi A, Ribas A. Tumour-intrinsic resistance to immune checkpoint blockade. *Nat Rev Immunol* 2020;20:25–39.

36 Pawlak M, DeTomaso D, Schnell A, *et al*. Induction of a colitogenic phenotype in Th1-like cells depends on interleukin-23 receptor signaling. *Immunity* 2022;55:1663–79.

37 Lo JW, Cozzetto D, Alexander JL, *et al*. Immune checkpoint inhibitor-induced colitis is mediated by polyfunctional lymphocytes and isdependent on anIL23/IFNγaxis. *Nat Commun* 2023;14:6719.

38 Thomas AS, McQuade J, Altan M, *et al*. S1778 IL12/23 blockade therapy for refractory immune checkpoint inhibitor colitis: a case series. *Am J Gastroenterol* 2021;116:S786.

39 Tang C, Chen S, Qian H, *et al*. Interleukin-23: as a drug target for autoimmune inflammatory diseases. *Immunology* 2012;135:112–24.

40 Wertheimer T, Zwicky P, Rindlisbacher L, *et al*. IL-23 stabilizes an effector $T_{reg}$ cell program in the tumor microenvironment. *Nat Immunol* 2024;25:512–24.

41 Oh DY, Cham J, Zhang L, *et al*. Immune toxicities elicted by CTLA-4 blockade in cancer patients are associated with early diversification of the T-cell Repertoire. *Cancer Res* 2017;77:1322–30.

42 Murray-Brown W, Wilsdon TD, Weedon H, *et al*. Nivolumab-induced synovitis is characterized by florid T cell infiltration and rapid resolution with synovial biopsy-guided therapy. *J Immunother Cancer* 2020;8:e000281.

43 Kotwal A, Gustafson MP, Bornschlegl S, *et al*. Immune checkpoint inhibitor-induced thyroiditis is associated with increased intrathyroidal T lymphocyte subpopulations. *Thyroid* 2020;30:1440–50.

44 Passat T, Touchefeu Y, Gervois N, *et al*. [Physiopathological mechanisms of immune-related adverse events induced by anti-CTLA-4, anti-PD-1 and anti-PD-L1 antibodies in cancer treatment]. *Bull Cancer* 2018;105:1033–41.

45 Quach HT, Dewan AK, Davis EJ, *et al*. Association of anti-programmed cell death 1 cutaneous toxic effects with outcomes in patients with advanced melanoma. *JAMA Oncol* 2019;5:906–8.

46 Rogado J, Sánchez-Torres JM, Romero-Laorden N, *et al*. Immune-related adverse events predict the therapeutic efficacy of anti–PD-1 antibodies in cancer patients. *Eur J Cancer* 2019;109:21–7.

47 Attia P, Phan GQ, Maker AV, *et al*. Autoimmunity correlates with tumor regression in patients with metastatic melanoma treated with anti-cytotoxic T-lymphocyte antigen-4. *J Clin Oncol* 2005;23:6043–53.

48 Zhou Y, Medik YB, Patel B, *et al*. Intestinal toxicity to CTLA-4 blockade driven by IL-6 and myeloid infiltration. *J Exp Med* 2023;220:e20221333.